Available online at http://scik.org

Commun. Math. Biol. Neurosci. 2025, 2025:138

https://doi.org/10.28919/cmbn/9556

ISSN: 2052-2541

MODELING AND ANALYSIS OF THE FOOD CHAIN'S DYNAMICS INCORPORATING FLOWERS, POLLINATORS, AND PREDATORS: THE ROLE OF ODORS

HUDA ABDUL SATAR[1], RAID KAMEL NAJI[2,*]

[1]Department of Mathematics, College of Science, University of Baghdad, Baghdad, Iraq

[2]Scientific Research Commission, Baghdad, Iraq

Abstract: For ecological interactions and plant reproduction, scents play a critical part in the food chain, which includes flowers, pollinators, and predators. Floral volatiles are important cues that attract pollinators, which in turn help plants reproduce. Additionally, these smells can affect predators and other higher trophic levels, thereby altering the dynamics of a community. To comprehend how the odor affects their dynamics, this work suggests and examines a food chain model of the aforementioned kind. The food chain model's stability analysis is examined locally with the help of linearization techniques and globally utilizing suitable Lyapunov functions. The possibility of local bifurcations occurring is examined, along with determining their kind using the Sotomayor theorem for local bifurcations. To validate the acquired analytical results and comprehend the influence of parameter values, a numerical simulation is performed.

Keywords: food chain; odor; stability; Lyapunov function; bifurcation.

2020 AMS Subject Classification: 92D30, 34D20, 34C23.

1. INTRODUCTION

In the disciplines of ecology, community biology, and computational biology, the prey-predator model has been thoroughly studied and applied. It helps scientists better grasp the factors influencing population dynamics and provides a lens through which to examine the complex

*Corresponding author

E-mail address: rknaji@src.edu.iq

Received August 16, 2025

relationships among various species. The model has been updated to include more elements, such as more complex community structures (food chains and food webs) and many environmental parameters including fear [1-3], refuge [4-6], harvesting [7-9], group defense [10-12], seasonality [13-15], cannibalism [16-18], Allee effect [19-21], infectious diseases [22-24], and many more others.

Thus, the classic Lotka-Volterra model was presented to build a prey-predator interaction centered on the Malthus growth rate [25, 26]. The Lotka-Volterra model is based on differential equations that describe the dynamics of populations of predators and prey. Over time, researchers have further developed and modified the model to include more realistic ecological scenarios [27–29] and the citations therein. The Lotka-Volterra framework is a fundamental concept in environmental modeling, despite its flaws, and that the real ecosystems are often more complex than the model predicts. It has made it possible to develop increasingly intricate models that aim to capture the intricacies of ecological systems. Because prey-predator interactions aid in understanding ecosystem dynamics and biodiversity, they remain an important field of study in ecology. For many years, scientists have been building many models to study the behaviors of this kind of ecological model and many other ecological scenarios [30–32].

As one organism consumes another, nutrients and energy go through the food chain, which is a linear arrangement of species. It symbolizes how matter and energy move through an environment. Since it enables us to recognize how ecosystems work and how human activity might impact them, an understanding of food chains is essential to ecology and environmental science [33]. The aforementioned makes it abundantly evident that food chains are an extension of the prey-predator system to higher levels, which are connected via the response function. From an ecological point of view, "functional response" describes the relationship between the number of prey and the rate at which a predator feeds on them [34]. It demonstrates how the presence of prey causes a consumer to alter the rate at which it feeds. Prey-dependent [35-36], predator-dependent [37-38], and ratio-dependent [39] are the three main categories that are employed. To make it more biologically realistic, a logistic growth term was employed for the prey species rather than a linear growth term. Functional responses play an important role in identifying population dynamics and prey-predator relationships in ecosystems. Ecologists and researchers can influence the overall stability and structure of ecological communities by simulating and predicting how predators affect prey populations and vice versa.

The majority of animals use odor to gather information, according to ecologists. For example, wolves use odor information to pursue prey [40], while female moths produce odor that contains unique enzymes to relay information [41]. Even though the sense of smell steadily deteriorates over animal evolution, it nevertheless plays a role in many different animal activities, including attracting enemies, foraging, stress reaction, and reproduction. Shen and Xue [42] examined the dynamics of the system and the impact of shelter on the prey population when predator odor was disrupted. Additionally, they used the Dulac-Bendixson principle to demonstrate the worldwide stability of the positive equilibrium point. The impact of odor disruption on the predator-prey relationship has not received much attention up to this point. Later on, a food chain model with collective defense and odor disruption was put up by Xu et al. [43]. In this model, prey are agitated by the smell of predators and band together to protect. However, Debasish et al. [44] investigated the effect of prey odor on predator population and, in turn, the food chain.

In contrast to the reviewed studies, this paper suggests a novel Lotka-Volterra food chain made up of flowers, pollinators, and predators to comprehend the effects of pollinator- and flower-induced odors on the dynamic behavior of the food chain. This is because there aren't many studies that focus on the role of odors in the dynamics of food chains in the environment. A multidisciplinary approach that combines biology, ecology, mathematics, and chemistry is the study of modeling and analysis of the dynamics of the food chain that includes flowers, pollinators, and predators, emphasizing the significance of scents. This field of study is essential for comprehending the complex interactions that exist within ecosystems and has broad ramifications for sustainable development, agriculture, and biodiversity protection. Moreover, Section 2 treats the model formulation. The dynamical behavior of the model is studied in Section 3. However, Section 4 solves the model numerically. Finally, the conclusion of our study is given in Section 5.

2. MATERIALS AND METHODS

Let that $x(t)$, $y(t)$, and $z(t)$ be the density of the flowers, pollinators, and predators at time t, respectively. The following biologically feasible assumptions are adopted to formulate the dynamics of such a food chain system.

The logistical expansion of flowers occurs when pollinators are scarce. The sweet scents released by flowers draw pollinators, including bees, butterflies, and birds. Pollinators visit flowers drawn by their scent to eat the nectar or gather pollen, which promotes the growth of the blooms. Because of their smell, these organisms may unintentionally draw pollinator-attracting predators to the

blooms, like spiders and insect-eating birds. Finally, pollinators and their predators decline exponentially in the absence of food.

Then, a set of 1st order differential equations can be used to explain the dynamics of such a food chain.

$$\begin{aligned}\frac{dx}{dt} &= \alpha x\left(1-\frac{x}{\beta}\right)-\gamma_1(1+\theta_1 x)xy+\gamma_2(1+\theta_1 x)xy = xg_1(x,y,z),\\ \frac{dy}{dt} &= e_1\gamma_1(1+\theta_1 x)xy-\mu(1+\theta_2 y)yz-d_1 y = yg_2(x,y,z),\\ \frac{dz}{dt} &= e_2\mu(1+\theta_2 y)yz-d_2 z = zg_3(x,y,z),\end{aligned} \tag{1}$$

where $x(0)\geq 0,\ y(0)\geq 0$, and $z(0)\geq 0$. All the system parameters are positive constants and stand for the rates as stated in Table 1.

Table 1: Parameter description

Parameter	Description
α	The intrinsic growth rate of the flower.
β	The environment-carrying capacity.
γ_1	The consume-nectar rate.
γ_2	The gather-pollen rate.
θ_1	The level of flower scents.
θ_2	The level of pollinator scents
μ	The predator consumption rate of pollinators
e_1	The conversion rate of flower nectar to pollinators' biomass
e_2	The conversion rate of pollinators' biomass to predator biomass
d_1, d_2	The mortality rates of pollinators and predators, respectively.

Since the growth functions $g_i, i=1,2,3$ belong to the set of functions C^1, hence system (1) with any nonnegative initial condition has a solution and is unique.

Therefore, when the value of $\gamma_2>\gamma_1$, the gather-pollen will help to grow the flower population. However, when the value $\gamma_2<\gamma_1$, this means the effect of the consume-nectar is stronger than the gather-pollen, and then the population of the flower will be decreased. Finally, when $\gamma_2=\gamma_1$, then the population of the flower will depend on the logistic growth only.

In the following theorem, the boundedness and positivity of solutions of the system (1) are established.

Theorem 1. *For any positive initial point with $\gamma_1(1-e_1)>\gamma_2$, the system's (1) solution is still positive and bounded for all time*.

Proof of Theorem 1. Consider the positive initial point $(x(0),y(0),z(0))$. Then from the flower

equation, it is obtained:

$$x(t) = x(0)\exp\left[\int_0^t \left(\alpha\left(1-\frac{x(s)}{\beta}\right) - \gamma_1\big(1+\theta_1 x(s)\big)y(s) + \gamma_2\big(1+\theta_1 x(s)\big)y(s)\right)ds\right] > 0.$$

Similarly, for the pollinators, and predators equations, it is obtained:

$$y(t) = y(0)\exp\left[\int_0^t \big(e_1\gamma_1\big(1+\theta_1 x(s)\big)x(s) - \mu\big(1+\theta_2 y(s)\big)z(s) - d_1\big)\,ds\right] > 0.$$

$$z(t) = z(0)\exp\left[\int_0^t \big(e_2\mu\big(1+\theta_2 y(s)\big)y(s) - d_2\big)\,ds\right] > 0.$$

Hence, by integrating the equations of system (1) using the positive initial point, it is obtained that the solution is still positive all the time according to the properties of the exponential function.

To prove the boundedness, the flower equation gives that:

$$\frac{dx}{dt} = \alpha x\left(1-\frac{x}{\beta}\right) - [\gamma_1-\gamma_2](1+\theta_1 x)xy \le \alpha x\left(1-\frac{x}{\beta}\right).$$

Therefore, by applying Lemma 2.2, [45], it was reached that:

$$x(t) \le \beta\,(1+(\beta x^{-1}(0)-1)e^{-\alpha t})^{-1}.$$

Therefore:

$$\lim_{t\to\infty} sup x(t) \le \beta.$$

Consider the function $\Lambda(t) = x(t) + y(t) + z(t)$ then:

$$\frac{\mathrm{d}\Lambda(t)}{dt} \le 2\alpha\beta - \alpha x - d_1 y - d_2 z \le 2\alpha\beta - \varsigma\Lambda,$$

where $\varsigma = \min\{\alpha, d_1, d_2\}$.

Therefore, utilizing Lemma 2.1, [45], yields that as $t\to\infty$ that $\sup\Lambda(t) \le \frac{\varsigma}{2\alpha\beta}$. Hence, the proof is complete.

Note that the nectar consumption rate is assumed to be higher than the pollen-gathering rate, as shown in Theorem 1, for keeping the population of the flowers bound; otherwise, it becomes unbounded, and this is what happens in nature.

The careful balance between this system of blooms, pollinators, and predators guarantees the existence of both plant and animal species. Pollinators aid in plant reproduction, the flowers give them food, and predators control pollinator populations to prevent any one species from taking over the environment. Each element is essential to preserving ecological health and biodiversity. There are many examples of such a system, from which Milkweed, Monarch Butterflies, and Birds;

Sunflowers, Bees, and Bee-eater Birds; Wild Blueberry Bushes, Bumblebees, and Robber Flies; and Apple Trees, Honey bees, and Hornets.

3. DYNAMICAL BEHAVIOR

For the components of this food chain to remain stable and continue to exist over time, it is crucial to comprehend the dynamic behavior of the flower-pollinators-predators food chain. The dynamic picture between these organisms may be complicated by the range of biological interactions found within the proposed food chain, such as the symbiosis between flowers and pollinators, the predation interaction between pollinators and predators, and the impact of odors from flowers and pollinators. Therefore, to research dynamic behavior, one must first identify the food chain's steady-state points (SSPs) system (1) and then investigate the dynamic behavior surrounding those points, including stability and bifurcation, as described in the following theories. Four SSPs have been identified in the system through a study; their forms and constraints are outlined below.

The vanishing-SSP (VSSP) is denoted by $\Gamma_1 = (0,0,0)$ and always exists.

The flower-SSP (FSSP) is denoted by $\Gamma_2 = (\beta, 0,0)$, and always exists.

The flower-pollinator-SSP (FPSSP) is denoted by $\Gamma_3 = (\bar{x}, \bar{y}, 0)$, where

$$\left.\begin{aligned} \bar{x} &= \frac{-e_1\gamma_1+\sqrt{e_1\gamma_1}\sqrt{e_1\gamma_1+4d_1\theta_1}}{2e_1\gamma_1\theta_1} \\ \bar{y} &= \frac{\alpha(\beta-\bar{x})}{\beta(\gamma_1-\gamma_2)(1+\theta_1\bar{x})} \end{aligned}\right\}. \tag{2}$$

It exists provided that the following constraint is satisfactory:

$$\gamma_2 < \gamma_1;\ \bar{x} < \beta. \tag{3}$$

The cohabitation-SSP (CSSP) is denoted by $\Gamma_3 = (\hat{x}, \hat{y}, \hat{z})$, where:

$$\left.\begin{aligned} \hat{y} &= \frac{-\mu e_2+\sqrt{\mu e_2}\sqrt{\mu e_2+4d_2\theta_2}}{2\mu e_2\theta_2} \\ \hat{x} &= \frac{\beta[\alpha-(\gamma_1-\gamma_2)\hat{y}]}{\alpha+\beta\theta_1(\gamma_1-\gamma_2)\hat{y}} \\ \hat{z} &= \frac{-d_1+e_1\gamma_1\hat{x}(1+\theta_1\hat{x})}{\mu(1+\theta_2\hat{y})} \end{aligned}\right\}. \tag{4}$$

It exists provided that the following constraint is satisfactory:

$$0 < (\gamma_1 - \gamma_2)\hat{y} < \alpha. \tag{5}$$

$$d_1 < e_1\gamma_1\hat{x}(1 + \theta_1\hat{x}). \tag{6}$$

Theorem 2. *The VSSP is a saddle point*.

Proof of Theorem 2. The Jacobian matrix (JM) at the VSSP can be determined as:

$$A(\Gamma_1) = \begin{bmatrix} \alpha & 0 & 0 \\ 0 & -d_1 & 0 \\ 0 & 0 & -d_2 \end{bmatrix}. \quad (7)$$

The eigenvalues are determined as $\alpha > 0$, $-d_1 < 0$, and $-d_2 < 0$. So, VSSP is a saddle point.

Theorem 3. *The FSSP is a sink under the following constraint*.

$$\beta e_1 \gamma_1 (1 + \beta\theta_1) < d_1. \quad (8)$$

It becomes globally stable under the constraint:

$$(\gamma_1 + \gamma_2)(1 + \theta_1\beta)\beta < d_1. \quad (9)$$

Moreover, system (1) undergoes a transcritical bifurcation (TB) near FSSP when:

$$\beta e_1 \gamma_1 (1 + \beta\theta_1) = d_1. \quad (10)$$

Proof of Theorem 3. The JM at the FSSP can be determined in the form:

$$A(\Gamma_2) = \begin{bmatrix} -\alpha & -\beta(\gamma_1 - \gamma_2)(1 + \beta\theta_1) & 0 \\ 0 & -d_1 + \beta e_1 \gamma_1 (1 + \beta\theta_1) & 0 \\ 0 & 0 & -d_2 \end{bmatrix}. \quad (11)$$

The eigenvalues are determined as $-\alpha < 0$, $-d_1 + \beta e_1 \gamma_1 (1 + \beta\theta_1)$, and $-d_2 < 0$. So, FSSP is a sink provided that the constraint (8) is satisfactory.

Consider, now the real-valued function $\mathrm{H}_1 = \int_\beta^x \frac{s-\beta}{s} ds + y + z$. It satisfies $\mathrm{H}_1(\beta, 0, 0) = 0$, and $\mathrm{H}_1(x, y, z) > 0$ for every point belonging to $\{x > 0, y \geq 0, z \geq 0\}$. Furthermore, direct computation gives that:

$$\frac{\mathrm{dH}_1}{dt} \leq -\frac{\alpha}{\beta}(x - \beta)^2 - [d_1 - (\gamma_1 + \gamma_2)(1 + \theta_1\beta)\beta]y - d_2 z.$$

Therefore, $\frac{\mathrm{dH}_1}{dt}$ becomes negative definite under the constraint (9), which leads to global stability.

When the constraint (10) is satisfactory, then $A(\Gamma_2, d_1)$ becomes:

$$A_1 = \begin{bmatrix} -\alpha & -\beta(\gamma_1 - \gamma_2)(1 + \beta\theta_1) & 0 \\ 0 & 0 & 0 \\ 0 & 0 & -d_2 \end{bmatrix}.$$

Then the eigenvalues of A_1 are $\lambda_x = -\alpha$, $\lambda_z = -d_2$, and $\lambda_y = 0$. Thus, the FSSP becomes a non-hyperbolic point. Let $\mathbf{U_1} = (v_{11}, v_{21}, v_{31})^T$ and $\mathbf{\Psi_1} = (\vartheta_{11}, \vartheta_{21}, \vartheta_{31})^T$ be the eigenvectors associated with the $\lambda_y = 0$ of the A_1 and ${A_1}^T$ respectively. Direct computation shows that $\mathbf{U_1} = \left(\frac{-\beta(\gamma_1 - \gamma_2)(1 + \beta\theta_1)}{\alpha}, 1, 0\right)^T = (\zeta_1, 1, 0)^T$ and $\mathbf{\Psi_1} = (0, 1, 0)^T$.

Using Sotomayor's theorem [46] gives that:

$$\frac{\partial \mathbf{G}}{\partial d_1}(\mathbf{Y}, d_1) = \begin{pmatrix} 0 \\ -y \\ 0 \end{pmatrix}, \text{ then } \mathbf{G}_{d_1}(\Gamma_2, d_1) = \begin{pmatrix} 0 \\ 0 \\ 0 \end{pmatrix},$$

where $\mathbf{G} = (xg_1, yg_2, zg_3)^{\mathrm{T}}, \mathbf{Y} = (x, y, z)^{\mathrm{T}}$**.** Therefore, $\boldsymbol{\Psi_1}^T \mathbf{G}_{d_1}(\Gamma_2, d_1) = 0$, and as a result, the first condition for TB is met. Moreover, since:

$$\boldsymbol{\Psi_1}^T D\mathbf{G}_{d_1}(\Gamma_2, d_1)\,\mathbf{U_1} = -1 \neq 0.$$

Also, direct computation gives that:

$$D^2\mathbf{G}(\Gamma_2, d_1)(\mathbf{U_1}, \mathbf{U_1}) = \begin{pmatrix} -2\zeta_1(\gamma_1 - \gamma_2)(1 + 2\theta_1\beta) - \frac{2\alpha{\zeta_1}^2}{\beta} \\ 2[e_1\zeta_1\gamma_1(1 + 2\theta_1\beta)] \\ 0 \end{pmatrix}.$$

As a result, the following is found:

$$\boldsymbol{\Psi_1}^T D^2\mathbf{G}(\Gamma_2, d_1)(\mathbf{U_1}, \mathbf{U_1}) = 2[e_1\zeta_1\gamma_1(1 + 2\theta_1\beta)] \neq 0.$$

Thus, a TB takes place around the FSSP.

Theorem 4. *The FPSSP is a sink under the following constraint*.

$$\mu e_2\bar{y}(1 + \theta_2\bar{y}) < d_2. \tag{12}$$

It is globally stable within a bounded domain of system (1) provided the following sufficient constraints are satisfied.

$$e_1\gamma_1\theta_1\bar{y}\bar{x} < (\gamma_1 - \gamma_2 - e_1\gamma_1\bar{y}), \tag{13}$$

$$e_1\gamma_1\beta(1 + \theta_1\beta) + \frac{1}{2} < d_1, \tag{14}$$

$$\mu(e_2 + \bar{y})(1 + \theta_2 y_{max})y_{max} < d_2, \tag{15}$$

$$\frac{[(\gamma_1 - \gamma_2 - e_1\gamma_1\bar{y})(1 + \theta_1\beta) - e_1\gamma_1\theta_1\bar{y}\bar{x}]^2}{2} < \frac{\alpha}{\beta} + (\gamma_1 - \gamma_2)\theta_1\bar{y}, \tag{16}$$

where y_{max} *represents the upper bound of* y *resulting from Theorem 1. Moreover, system (1) undergoes a TB at FPSSP when the following constraint holds*:

$$\mu e_2\bar{y}(1 + \theta_2\bar{y}) = d_2. \tag{17}$$

Proof of Theorem 4. The JM at the PFSSP can be calculated as:

$$A(\Gamma_3) = \begin{bmatrix} -\bar{x}\left(\frac{\alpha}{\beta} + \theta_1(\gamma_1 - \gamma_2)\bar{y}\right) & -\bar{x}(\gamma_1 - \gamma_2)(1 + \theta_1\bar{x}) & 0 \\ e_1\gamma_1\bar{y}(1 + 2\theta_1\bar{x}) & 0 & -\mu\bar{y}(1 + \theta_2\bar{y}) \\ 0 & 0 & -d_2 + \mu e_2\bar{y}(1 + \theta_2\bar{y}) \end{bmatrix}. \tag{18}$$

The characteristic equation of $A(\Gamma_3)$ can be written as:

$$\left[\lambda^2 + \bar{x}\left(\frac{\alpha}{\beta} + \theta_1(\gamma_1 - \gamma_2)\bar{y}\right)\lambda + e_1\gamma_1\bar{x}\bar{y}(\gamma_1 - \gamma_2)(1 + \theta_1\bar{x})(1 + 2\theta_1\bar{x})\right]$$
$$[-d_2 + \mu e_2\bar{y}(1 + \theta_2\bar{y}) - \lambda] = 0.$$

From the RH criterion, it is easy to verify that there are two negative real parts eigenvalues given by:

$$\lambda_{31},\lambda_{32}=\frac{-\bar{x}\left(\frac{\alpha}{\beta}+\theta_1(\gamma_1-\gamma_2)\bar{y}\right)}{2}$$
$$\pm\frac{1}{2}\sqrt{\bar{x}^2\left(\frac{\alpha}{\beta}+\theta_1(\gamma_1-\gamma_2)\bar{y}\right)^2-4e_1\gamma_1\bar{x}\bar{y}(\gamma_1-\gamma_2)(1+\theta_1\bar{x})(1+2\theta_1\bar{x})}.$$

While the third eigenvalue is $\lambda_{33}=-d_2+\mu e_2\bar{y}(1+\theta_2\bar{y})$. Therefore, the FPSSP is a sink under the constraint (12).

Consider, now the real-valued function $\mathrm{H}_2=\int_{\bar{x}}^{x}\frac{s-\bar{x}}{s}ds+\frac{(y-\bar{y})^2}{2}+z$. It satisfies $\mathrm{H}_2(\bar{x},\bar{y},0)=0$, and $\mathrm{H}_2(x,y,z)>0$ for every point belonging to $\{x>0,y>0,z\geq 0\}$. Furthermore, direct computation gives that:

$$\begin{aligned}\frac{\mathrm{dH}_2}{\mathrm{dt}}=&-\left[\frac{\alpha}{\beta}+(\gamma_1-\gamma_2)\theta_1\bar{y}\right](x-\bar{x})^2-[d_1-e_1\gamma_1x(1+\theta_1x)](y-\bar{y})^2\\&-[(\gamma_1-\gamma_2-e_1\gamma_1\bar{y})(1+\theta_1x)-e_1\gamma_1\theta_1\bar{y}\bar{x}](x-\bar{x})(y-\bar{y})\\&-\mu(y-\bar{y})(1+\theta_2y)yz+e_2\mu(1+\theta_2y)yz-d_2z.\end{aligned}$$

Further simplifying yields that:

$$\begin{aligned}\frac{\mathrm{dH}_2}{dt}\leq&-\left[\frac{\alpha}{\beta}+(\gamma_1-\gamma_2)\theta_1\bar{y}-\frac{M^2}{2}\right](x-\bar{x})^2-\left[d_1-e_1\gamma_1x(1+\theta_1x)-\frac{1}{2}\right](y-\bar{y})^2\\&-[d_2-\mu(e_2+\bar{y})(1+\theta_2y)y]z,\end{aligned}$$

where $M=(\gamma_1-\gamma_2-e_1\gamma_1\bar{y})(1+\theta_1x)-e_1\gamma_1\theta_1\bar{y}\bar{x}$. Hence, using the constraints (13)-(16) makes $\frac{\mathrm{dH}_2}{dt}$ negative definite and leads to global stability.

When the constraint (17) is satisfactory, then $A(\Gamma_3,d_2)$ that given in (18) becomes:

$$A_2=\begin{bmatrix}-\bar{x}\left(\frac{\alpha}{\beta}+\theta_1(\gamma_1-\gamma_2)\bar{y}\right) & -\bar{x}(\gamma_1-\gamma_2)(1+\theta_1\bar{x}) & 0\\ e_1\gamma_1\bar{y}(1+2\theta_1\bar{x}) & 0 & -\mu\bar{y}(1+\theta_2\bar{y})\\ 0 & 0 & 0\end{bmatrix}.$$

The eigenvalues of A_2 are given by $\lambda_{31},\lambda_{32}$, and $\lambda_z=0$. Thus, the FPSSP is a non-hyperbolic point. Let $\mathbf{U_2}=(v_{12},v_{22},v_{32})^T$ and $\mathbf{\Psi_2}=(\vartheta_{12},\vartheta_{22},\vartheta_{32})^T$ be the eigenvectors corresponding to $\lambda_z=0$ of the A_2 and ${A_2}^T$ respectively. Direct computation shows that $\mathbf{U_2}=(\zeta_2,\zeta_3,1)^T$, and $\mathbf{\Psi_2}=(0,0,1)^T$, where:

$$\zeta_2=\frac{\mu(1+\theta_2\bar{y})}{e_1\gamma_1(1+2\theta_1\bar{x})}\text{ and }\zeta_3=-\frac{\mu\left(\frac{\alpha}{\beta}+\theta_1(\gamma_1-\gamma_2)\bar{y}\right)(1+\theta_2\bar{y})}{e_1\gamma_1(\gamma_1-\gamma_2)(1+\theta_1\bar{x})(1+2\theta_1\bar{x})}.$$

Now, it is observed that:

$$\frac{\partial\mathbf{G}}{\partial d_2}(\mathbf{Y},d_2)=\begin{pmatrix}0\\0\\-z\end{pmatrix},\text{ then }\mathbf{G}_{d_2}(\Gamma_3,d_2)=\begin{pmatrix}0\\0\\0\end{pmatrix}.$$

Therefore, ${\mathbf{\Psi_2}}^T\mathbf{G}_{d_2}(\Gamma_3,d_2)=0$, the first condition for TB is met. Moreover, since:

$${\mathbf{\Psi_2}}^T D\mathbf{G}_{d_2}(\Gamma_3,d_2)\,\mathbf{U_2}=-1\neq 0.$$

Furthermore, direct computation gives that:

$$D^2\mathbf{G}(\Gamma_3, d_2)(\mathbf{U_2}, \mathbf{U_2}) = \begin{pmatrix} -2\zeta_2\zeta_3(\gamma_1-\gamma_2)(1+2\theta_1\bar{x}) - \frac{2{\zeta_2}^2(\alpha+\beta(\gamma_1-\gamma_2)\theta_1\bar{y})}{\beta} \\ 2\big(e_1{\zeta_2}^2\gamma_1\theta_1\bar{y} + \zeta_3[e_1\zeta_2\gamma_1(1+2\theta_1\bar{x}) - \mu(1+2\theta_2\bar{y})]\big) \\ 2\mu e_2\zeta_3(1+2\theta_2\bar{y}) \end{pmatrix}.$$

So, the following is found:

$${\mathbf{\Psi_2}}^T D^2\mathbf{G}(\Gamma_3, d_2)(\mathbf{U_2}, \mathbf{U_2}) = 2\mu e_2\zeta_3(1+2\theta_2\bar{y}) \neq 0.$$

Then a TB takes place around the FPSSP.

Theorem 5. *The CSSP is an unconstrained sink. It becomes globally stable when the following sufficient constraints are satisfied*.

$$e_1\gamma_1\theta_1\hat{x} < (\gamma_1-\gamma_2-e_1\gamma_1), \tag{19}$$

$$e_2(1+\theta_2 y_{max}+\theta_2\hat{y})z_{max} < 1, \tag{20}$$

$$\frac{[(\gamma_1-\gamma_2-e_1\gamma_1)(1+\theta_1\beta)-e_1\gamma_1\theta_1\hat{x}]^2}{2} < \frac{\alpha}{\beta} + (\gamma_1-\gamma_2)\theta_1\hat{y}, \tag{21}$$

$$\frac{1}{2}([\mu(1+\theta_2 y_{max})]^2+1) < \mu\theta_2\hat{z}. \tag{22}$$

$$e_2\mu\hat{y}(1+\theta_2\hat{y}) + \frac{1}{2} < d_2. \tag{23}$$

Proof of Theorem 5. The JM at the CSSP can be determined by:

$$A(\Gamma_4) = \begin{bmatrix} -\hat{x}\left[\frac{\alpha}{\beta}+\theta_1\hat{y}(\gamma_1-\gamma_2)\right] & -\hat{x}(\gamma_1-\gamma_2)(1+\theta_1\hat{x}) & 0 \\ e_1\gamma_1\hat{y}(1+2\theta_1\hat{x}) & -\mu\hat{y}\hat{z}\theta_2 & -\mu\hat{y}(1+\theta_2\hat{y}) \\ 0 & \mu e_2\hat{z}(1+2\theta_2\hat{y}) & 0 \end{bmatrix}.$$

Therefore, the characteristic equation of $A(\Gamma_4)$ can be written as:

$$\lambda^3 + \Sigma_1\lambda^2 + \Sigma_2\lambda + \Sigma_3 = 0,$$

where

$$\Sigma_1 = \hat{x}\left[\frac{\alpha}{\beta}+\theta_1\hat{y}(\gamma_1-\gamma_2)\right] + \mu\hat{y}\hat{z}\theta_2 > 0,$$

$$\Sigma_2 = \mu\theta_2\hat{x}\hat{y}\hat{z}\left[\frac{\alpha}{\beta}+\theta_1\hat{y}(\gamma_1-\gamma_2)\right] + e_1\gamma_1\hat{x}\hat{y}(\gamma_1-\gamma_2)(1+\theta_1\hat{x})(1+2\theta_1\hat{x}) + \mu^2 e_2\hat{y}\hat{z}(1+\theta_2\hat{y})(1+2\theta_2\hat{y}) > 0.$$

$$\Sigma_3 = \mu^2 e_2\hat{x}\hat{y}\hat{z}\left[\frac{\alpha}{\beta}+\theta_1\hat{y}(\gamma_1-\gamma_2)\right](1+\theta_2\hat{y})(1+2\theta_2\hat{y}) > 0.$$

Moreover, it is obtained that

$$\Sigma_1\Sigma_2 - \Sigma_3 = \mu\hat{y}\hat{z}\theta_2\Sigma_2 + \mu\theta_2\hat{x}^2\hat{y}\hat{z}\left[\frac{\alpha}{\beta}+\theta_1\hat{y}(\gamma_1-\gamma_2)\right]^2 + e_1\gamma_1\hat{x}^2\hat{y}(\gamma_1-\gamma_2)(1+\theta_1\hat{x})(1+2\theta_1\hat{x})\left[\frac{\alpha}{\beta}+\theta_1\hat{y}(\gamma_1-\gamma_2)\right] > 0.$$

Consequently, due to the RH criterion, CSSP is an unconstrained sink.

Define now the real-valued function $\mathrm{H}_3 = \int_{\hat{x}}^{x} \frac{s-\hat{x}}{s} ds + \int_{\hat{y}}^{y} \frac{s-\hat{y}}{s} ds + \frac{(z-\hat{z})^2}{2}$. It satisfies $\mathrm{H}_3(\hat{x}, \hat{y}, \hat{z}) = 0$, and $\mathrm{H}_3(x, y, z) > 0$ for every point belonging to $\{x > 0, y > 0, z > 0\}$. Furthermore, direct computation gives that:

$$\frac{d\mathrm{H}_3}{dt} = -\left[\frac{\alpha}{\beta} + (\gamma_1 - \gamma_2)\theta_1\hat{y}\right](x-\hat{x})^2 - [d_2 - e_2\mu\hat{y} - e_2\mu\theta_2\hat{y}^2](z-\hat{z})^2$$
$$-\mu\theta_2\hat{z}(y-\hat{y})^2 - [(\gamma_1 - \gamma_2 - e_1\gamma_1)(1+\theta_1 x) - e_1\gamma_1\theta_1\hat{x}](x-\hat{x})(y-\hat{y})$$
$$-[\mu(1+\theta_2 y) - e_2\mu(1+\theta_2 y + \theta_2\hat{y})z](y-\hat{y})(z-\hat{z}).$$

Further simplifying yields that:

$$\frac{d\mathrm{H}_3}{dt} < -\left[\frac{\alpha}{\beta} + (\gamma_1 - \gamma_2)\theta_1\hat{y}\right](x-\hat{x})^2 - [d_2 - e_2\mu\hat{y} - e_2\mu\theta_2\hat{y}^2](z-\hat{z})^2$$
$$-\mu\theta_2\hat{z}(y-\hat{y})^2 + \frac{{Q_1}^2}{2}(x-\hat{x})^2 + \frac{1}{2}(y-\hat{y})^2$$
$$+\frac{{Q_2}^2}{2}(y-\hat{y})^2 + \frac{1}{2}(z-\hat{z})^2.$$

Consequently, it follows:

$$\frac{d\mathrm{H}_3}{dt} < -\left[\frac{\alpha}{\beta} + (\gamma_1 - \gamma_2)\theta_1\hat{y} - \frac{{Q_1}^2}{2}\right](x-\hat{x})^2 - \left[\mu\theta_2\hat{z} - \frac{1}{2}({Q_2}^2 + 1)\right](y-\hat{y})^2$$
$$-\left[d_2 - e_2\mu\hat{y} - e_2\mu\theta_2\hat{y}^2 - \frac{1}{2}\right](z-\hat{z})^2,$$

where $Q_1 = (\gamma_1 - \gamma_2 - e_1\gamma_1)(1+\theta_1 x) - e_1\gamma_1\theta_1\hat{x}$, and $Q_2 = \mu(1+\theta_2 y) - e_2\mu(1+\theta_2 y + \theta_2\hat{y})z$. Hence, using the constraints (19)-(23) makes $\frac{\mathrm{dH}_3}{dt}$ negative definite, and that leads to global stability.

Note that, since the CSSP is a structurally stable local bifurcation in the sense of Sotomayor and Hopf bifurcation cannot occur.

4. NUMERICAL SIMULATION

Because ecological systems are complex and dynamic, numerical simulation is an effective tool for studying them. For ecologists to comprehend, forecast, and effectively manage complex ecological systems, it is a flexible and indispensable tool. To accomplish this, system (1) is solved numerically using the hypothetical set of parameter values listed below, beginning from various initial points that are part of the system domain.

$$\alpha = 2, \beta = 20, \gamma_1 = 0.2, \gamma_2 = 0.1, \theta_1 = 0.05, \theta_2 = 0.15,$$
$$e_1 = 0.2, e_2 = 0.2, d_1 = 0.1, d_2 = 0.2, \mu = 0.1. \quad (24)$$

It is observed that the system (1) solutions converge to $\Gamma_4 = (\hat{x}, \hat{y}, \hat{z}) = (11.39, 5.48, 3.37)$ starting from different points, as shown in Figure 1.

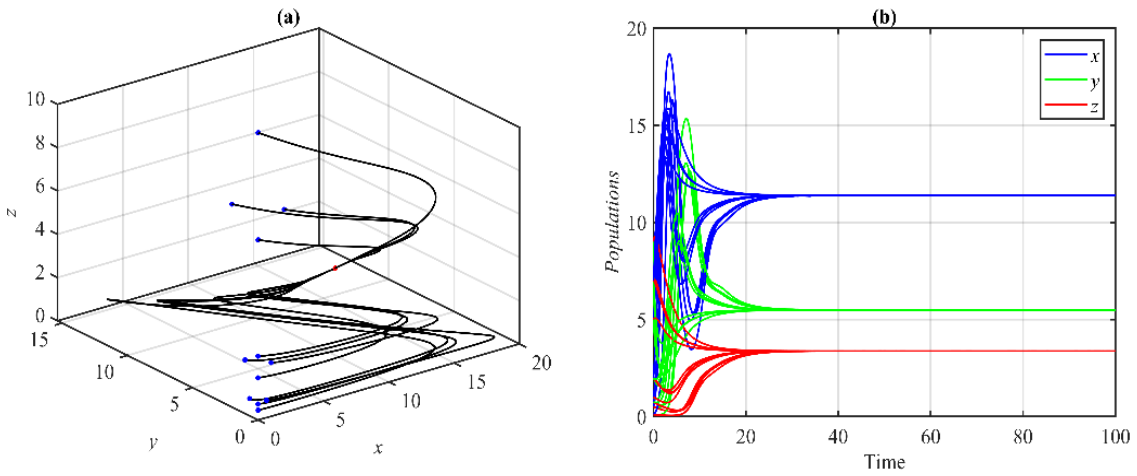

Figure 1: Using the set (24) with different initial points, the system (1) solutions converge to $\Gamma_4 = (\hat{x}, \hat{y}, \hat{z}) = (11.39, 5.48, 3.37)$. (a) 3D Orbits. (b) Solutions as a function of time.

From Figure 1 it can be concluded that system (1) has globally asymptotically stable CSSP, which shows that all three populations in the proposed food chain are in a stable SSP at CSSP, which means that their densities don't go extinct or increase out of control over time. Now, it is verified that for $\alpha \leq 0.688$, and $0.688 < \alpha$, the solution of system (1) attracts to Γ_3 and Γ_4, respectively; see for explanation Figure 2. This indicates the existence of one bifurcation value in the range of α once the parameter exceeds that value, the system becomes globally asymptotically stable at CSSP. Similar results were obtained as shown with increasing α when the parameters e_1, e_2, and μ increase.

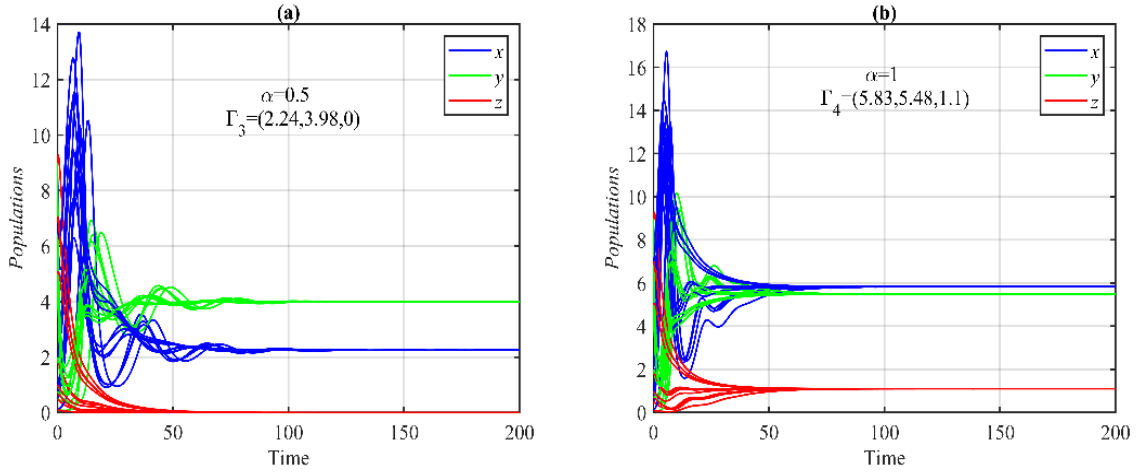

Figure 2: Using the set (24) with different initial points, the time series of the system (1) solution: (a) Attracting to Γ_3 when $\alpha = 0.5$. (b) Attracting to Γ_4 when $\alpha = 1$.

Figure 2 indicates that reducing the intrinsic growth rate of the flower or any of the conversion

rates or predator consumption rate of pollinators causes extinction in the predator.

For $\beta \leq 2$, $2 < \beta < 3.3$, and $3.3 \leq \beta$, it is confirmed numerically that the solutions attract to Γ_2, Γ_3, and Γ_4, respectively, as explained in Figure 3.

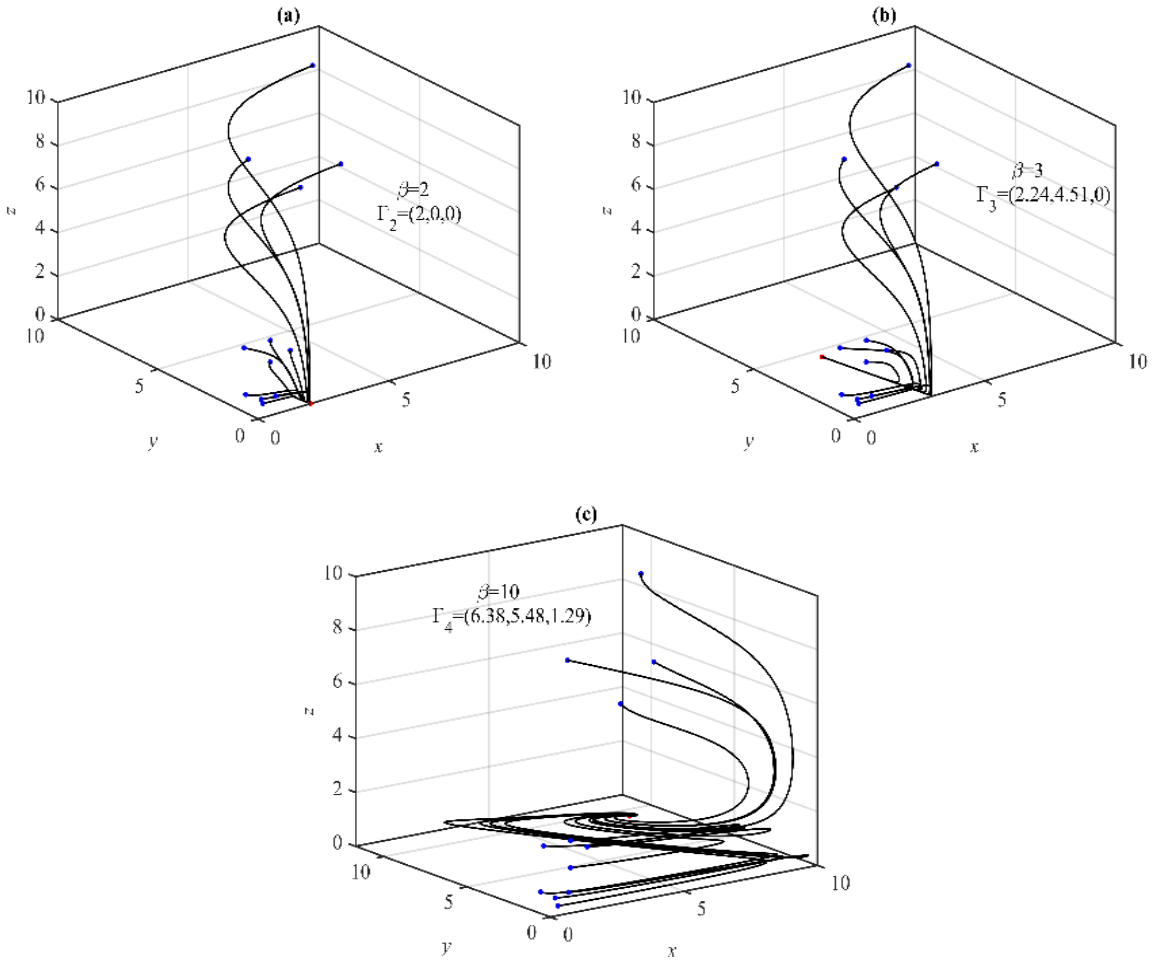

Figure 3: Using the set (24) with different initial points, a 3D Phase portrait of a system (1). (a) Γ_2 is globally asymptotically stable when $\beta = 2$. (b) Γ_3 is globally asymptotically stable when $\beta = 3$. (c) Γ_4 is globally asymptotically stable when $\beta = 10$.

As shown in Figure 3, the range of β contains two bifurcation values. Once the value of β increases and passes through the first one the solution changes its stability from Γ_2 to Γ_3 and then to Γ_4 after passing the second bifurcation value, which refers to stabilizing the system. Therefore, reducing the environment-carrying capacity leads to disappearing of both the populations of pollinators, and predators from the environment.

Now, the numerical results show that the solution exchanges its stability from Γ_4 to Γ_3 once the parameter γ_1 increases and passes through the value $\gamma_1 = 0.44$ as presented in Figure 4. Similar

results were obtained as shown with increasing γ_1 when the parameters θ_1 and d_2 increase. The trade-off between the existence of nectar/pollen rewards and the allure of floral scents determines how long the flower-pollinator relationship will last. Pollinators may not locate flowers if scents are too faint or deceptive, which would interfere with pollination and decrease flower reproduction. As a result, the system gets closer to the FPSSP when the predator faces extinction due to an increase in flowery scents.

Moreover, it is obtained that changing the parameters γ_2 and θ_2 has a quantitative influence on the dynamics of the system (1), in which the position of CSSP is moving but still attracting all the solutions, see Figures 5 and 6. It is verified that for the large values of $\gamma_2 > 0.22$, the system loses its bounds.

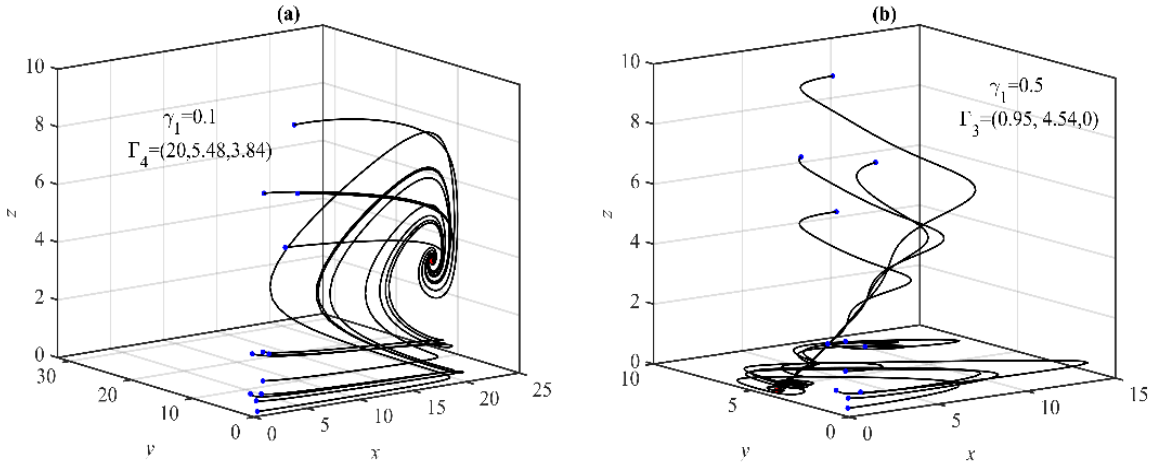

Figure 4: Using the set (24) with different initial points, 3D orbits of a system (1). (a) Γ_4 is globally asymptotically stable when $\gamma_1 = 0.1$. (b) Γ_3 is globally asymptotically stable when $\gamma_1 = 0.5$.

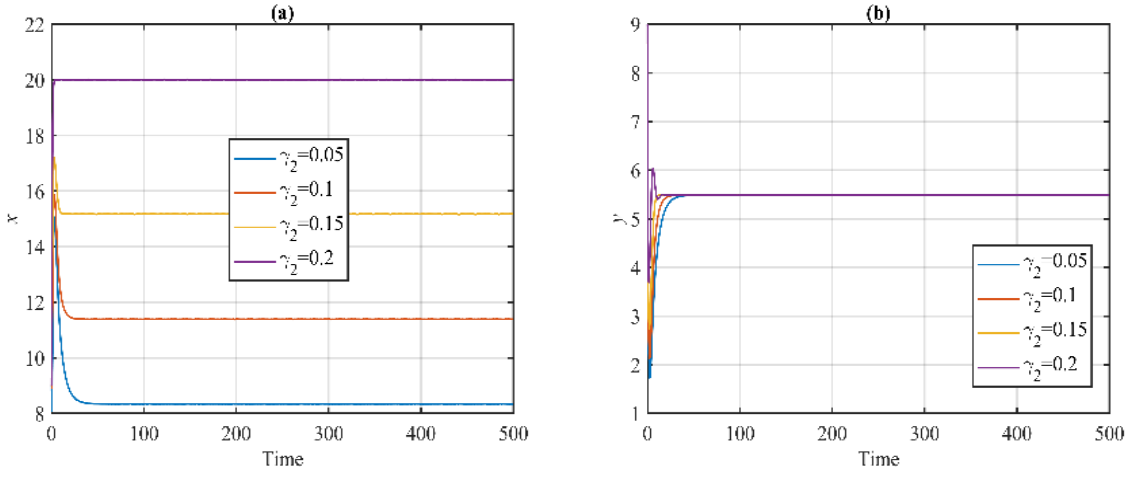

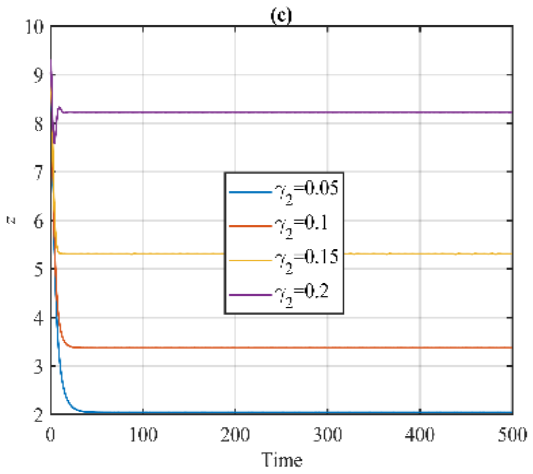

Figure 5: Using the set (24) with different values of γ_2, the time series of the system (1) solution: (a) The orbits of x as a function of time. (b) The orbits of y as a function of time. (c) The orbits z as a function of time.

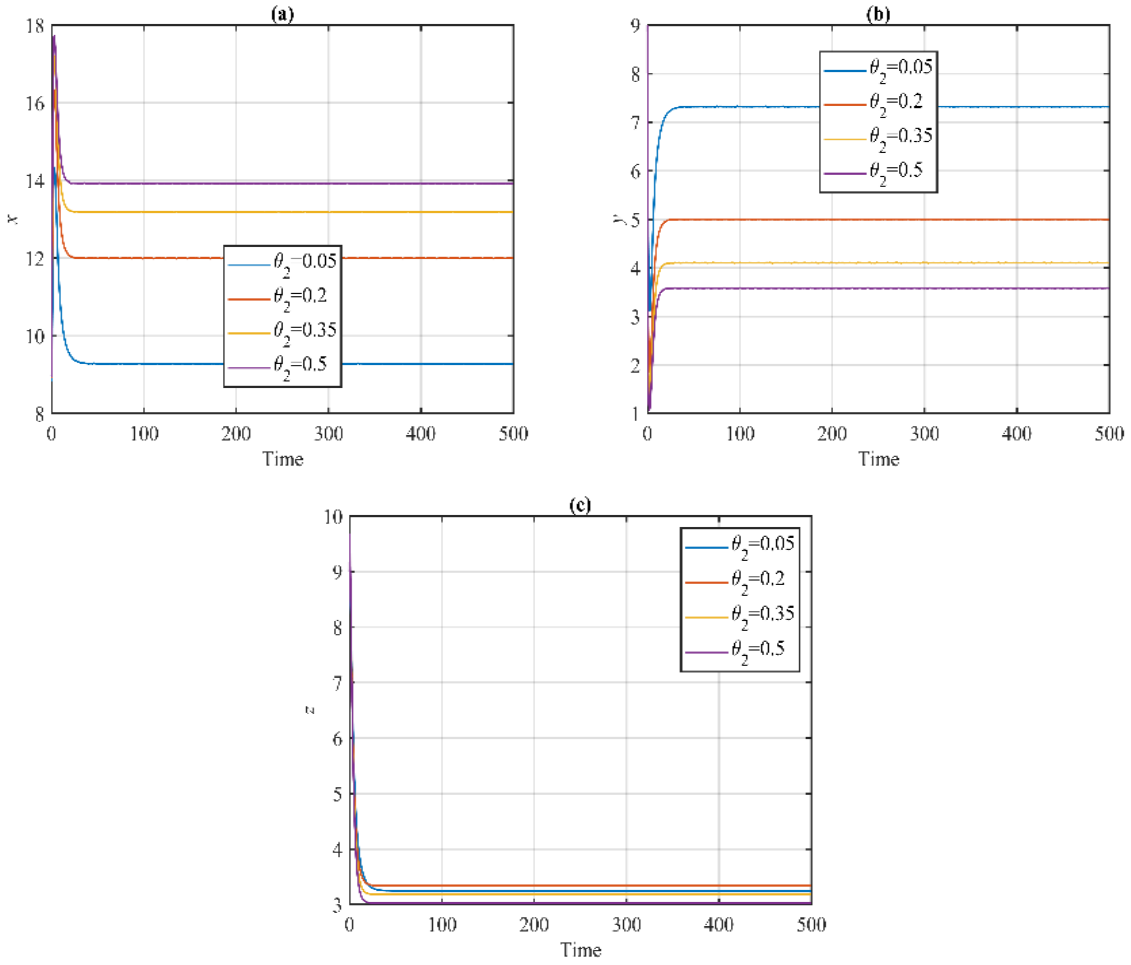

Figure 6: Using the set (24) with different values of θ_2, the time series of the system (1) solution: (a) The orbits of x as a function of time. (b) The orbits of y as a function of time. (c) The orbits

z as a function of time.

It is clear from Figure 5 that both the populations x and z are increasing with an increase in γ_2, while y is unaffected. However, Figure 6 reflects that an increase in the population of x and a decrease in both the populations of y and z occur when the value of θ_2 is raised. Finally, for $d_1 \leq 0.72$, $0.72 < d_1 < 1.6$, and $1.6 \leq d_1$, the solutions attract to Γ_4, Γ_3, and Γ_2 respectively, as explained in Figure 7. This referred to the bifurcation occurrence at two bifurcation points in the range of d_1 in addition to losing the persistence of the system (1) with the increase of d_1.

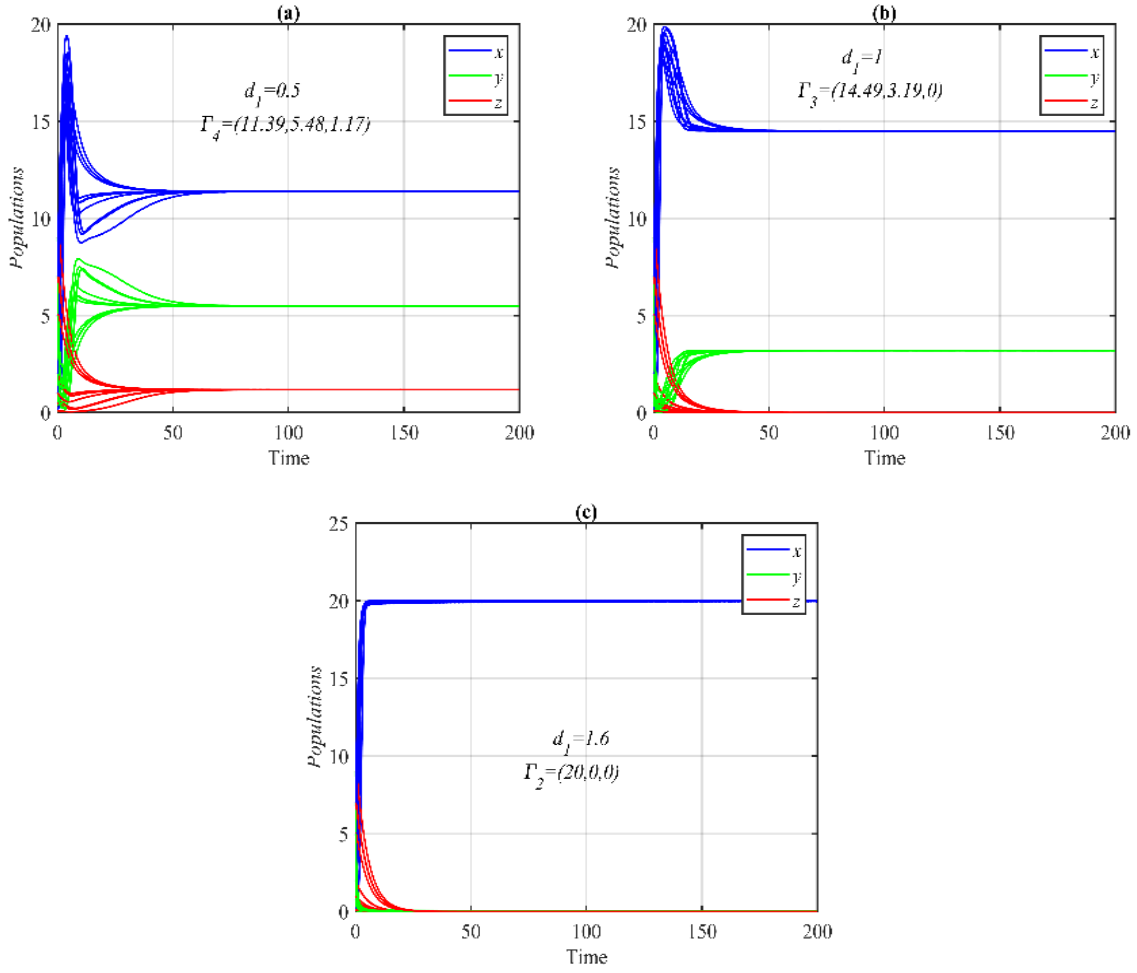

Figure 7: Using the set (24) with different initial points, the time series of the system (1) solution: (a) Attracting to Γ_4 when $d_1 = 0.5$. (b) Attracting to Γ_3 when $d_1 = 1$. (c) Attracting to Γ_2 when $d_1 = 1.6$.

5. CONCLUSION

This work presents a mathematical simulation of a three-species food chain model that includes flowers, pollinators, and predators. Odors' function in this food chain's dynamics is examined and taken into account. A system of ordinary differential equations is used to formulate the dynamic behavior of this food chain. Stability analyses are examined both locally and globally to better understand the intricate relationships forming this ecosystem. To determine their impact on the dynamic system of the food chain, the role of scents and other characteristics is examined through numerical simulation and bifurcation analysis. It is observed that four potential nonnegative SSPs function as attracting the food chain's final state based on specific conditions.

From an alternative perspective, the following outcomes are obtained from the numerical simulation using a fictitious set of parameter values provided by (24). Every analytical result that was acquired has been verified. Instead of having periodic dynamics, the system trades stability with the SSPs. The dynamic of the system at the CSSP is confirmed to be stabilized by an increase in the values of the flower growth rate, environment-carrying capacity, pollinator predator consumption rate, flower nectar conversion rate to pollinator biomass, or pollinator biomass conversion rate to predator biomass. However, extinction in predator species results from increases in the consume-nectar rate, floral fragrance levels, or predator death rates. This means that the food chain model's persistence is lost, and their solution approaches FPSSP. Furthermore, the system converges to FSSP when pollinator mortality rates rise above a particular threshold. Lastly, the pollinator death rate and environmental carrying capacity values have the opposite impact on the food chain's dynamics, indicating that the food chain is highly susceptible to these parameters.

An essential feature of ecological and biological systems is memory. Instead of utilizing the classical temporal derivative utilized in this manuscript, it would be interesting to employ the novel Hattaf generalized fractional derivative and fractal-fractional derivative developed in [47–48] to examine the memory effect on the dynamics of our suggested model in future work. Moreover, the proposed model can be studied under the effect of delay in the response of the odor effect.

CONFLICT OF INTERESTS

The authors declare that there is no conflict of interests.

REFERENCES

[1] X. Wang, L. Zanette, X. Zou, Modelling the Fear Effect in Predator–Prey Interactions, J. Math. Biol. 73 (2016), 1179-1204. https://doi.org/10.1007/s00285-016-0989-1.

[2] H. Wu, Z. Li, M. He, Dynamic Analysis of a Leslie-Gower Predator-Prey Model with the Fear Effect and Nonlinear Harvesting, Math. Biosci. Eng. 20 (2023), 18592-18629. https://doi.org/10.3934/mbe.2023825.

[3] F.H. Maghool, R.K. Naji, The Dynamics of a Tritrophic Leslie-Gower Food-Web System with the Effect of Fear, J. Appl. Math. 2021 (2021), 2112814. https://doi.org/10.1155/2021/2112814.

[4] J. Ghosh, B. Sahoo, S. Poria, Prey-Predator Dynamics with Prey Refuge Providing Additional Food to Predator, Chaos Solitons Fractals 96 (2017), 110-119. https://doi.org/10.1016/j.chaos.2017.01.010.

[5] A.R.M. Jamil, R.K. Naji, Modeling and Analysis of the Influence of Fear on the Harvested Modified Leslie–Gower Model Involving Nonlinear Prey Refuge, Mathematics 10 (2022), 2857. https://doi.org/10.3390/math10162857.

[6] Z.M. Hadi, D.K. Bahlool, The Effect of Alternative Resource and Refuge on the Dynamical Behavior of Food Chain Model, Malays. J. Math. Sci. 17 (2023), 731-754. https://doi.org/10.47836/mjms.17.4.13.

[7] D.K. Bahlool, H.A. Satar, H.A. Ibrahim, Order and Chaos in a Prey-Predator Model Incorporating Refuge, Disease, and Harvesting, J. Appl. Math. 2020 (2020), 5373817. https://doi.org/10.1155/2020/5373817.

[8] H.A. Satar, R.K. Naji, Stability and Bifurcation in a Prey–Predator–Scavenger System with Michaelis–Menten Type of Harvesting Function, Differ. Equ. Dyn. Syst. 30 (2019), 933-956. https://doi.org/10.1007/s12591-018-00449-5.

[9] C. Lu, X. Liu, Z. Li, The Dynamics and Harvesting Strategies of a Predator-Prey System with Allee Effect on Prey, AIMS Math. 8 (2023), 28897-28925. https://doi.org/10.3934/math.20231481.

[10] S.K. Sasmal, Y. Takeuchi, Dynamics of a Predator-Prey System with Fear and Group Defense, J. Math. Anal. Appl. 481 (2020), 123471. https://doi.org/10.1016/j.jmaa.2019.123471.

[11] S. Pal, S. Karmakar, S. Pal, N. Pal, A.K. Misra, et al., Impact of Fear and Group Defense on the Dynamics of a Predator–Prey System, Int. J. Bifurc. Chaos 34 (2024), 2450019. https://doi.org/10.1142/s0218127424500196.

[12] Y. Yao, L. Liu, Dynamics of a Predator–Prey System with Foraging Facilitation and Group Defense, Commun. Nonlinear Sci. Numer. Simul. 138 (2024), 108198. https://doi.org/10.1016/j.cnsns.2024.108198.

[13] D. Barman, S. Roy, P.K. Tiwari, S. Alam, Two-Fold Impacts of Fear in a Seasonally Forced Predator–Prey System with Cosner Functional Response, J. Biol. Syst. 31 (2023), 517-555. https://doi.org/10.1142/s0218339023500183.

[14] D. Barman, R.K. Upadhyay, Modelling Predator–Prey Interactions: A Trade-Off Between Seasonality and Wind Speed, Mathematics 11 (2023), 4863. https://doi.org/10.3390/math11234863.

[15] J. Alebraheem, Rich Dynamics of Seasonal Carrying Capacity Prey-Predator Models with Crowley–Martin Functional Response, Math. Comput. Appl. 30 (2025), 11. https://doi.org/10.3390/mca30010011.

[16] H.A. Ibrahim, R.K. Naji, The Complex Dynamic in Three Species Food Webmodel Involving Stage Structure and Cannibalism, AIP Conf. Proc. 2292 (2020), 020006. https://doi.org/10.1063/5.0030510.

[17] R. Lavanya, S. Vinoth, K. Sathiyanathan, Z. Njitacke Tabekoueng, P. Hammachukiattikul, et al., Dynamical Behavior of a Delayed Holling Type-II Predator-Prey Model with Predator Cannibalism, J. Math. 2022 (2022), 4071375. https://doi.org/10.1155/2022/4071375.

[18] M. Rayungsari, A. Suryanto, W.M. Kusumawinahyu, I. Darti, Dynamical Analysis of a Predator-Prey Model Incorporating Predator Cannibalism and Refuge, Axioms 11 (2022), 116. https://doi.org/10.3390/axioms11030116.

[19] S. Al-Momen, R.K. Naji, The Dynamics of Sokol-Howell Prey-Predator Model Involving Strong Allee Effect, Iraqi J. Sci. 62 (2021), 3114-3127. https://doi.org/10.24996/ijs.2021.62.9.27.

[20] F. Wang, R. Yang, Y. Xie, J. Zhao, Hopf Bifurcation in a Delayed Reaction Diffusion Predator-Prey Model with Weak Allee Effect on Prey and Fear Effect on Predator, AIMS Math. 8 (2023), 17719-17743. https://doi.org/10.3934/math.2023905.

[21] N. Min, H. Zhang, X. Gao, P. Zeng, Impacts of Hunting Cooperation and Prey Harvesting in a Leslie-Gower Prey-Predator System with Strong Allee Effect, AIMS Math. 9 (2024), 34618-34646. https://doi.org/10.3934/math.20241649.

[22] Walaa Madhat Alwan, Huda Abdul Satar, The Effects of Media Coverage on the Dynamics of Disease in Prey-Predator Model, Iraqi J. Sci. 62 (2021), 981-996. https://doi.org/10.24996/ijs.2021.62.3.28.

[23] M. Wang, S. Yao, The Dynamics of an Eco-Epidemiological Prey–Predator Model with Infectious Diseases in Prey, Commun. Nonlinear Sci. Numer. Simul. 132 (2024), 107902. https://doi.org/10.1016/j.cnsns.2024.107902.

[24] K.G. Mekonen, A.F. Bezabih, K.P. Rao, Mathematical Modeling of Infectious Disease and Prey-Predator Interaction with Optimal Control, Int. J. Math. Math. Sci. 2024 (2024), 5444627. https://doi.org/10.1155/2024/5444627.

[25] A.J. Lotka, Elements of Physical Biology, Williams and Wilkins Company, Baltimore, (1925).

[26] V. Volterra, Variations and Fluctuations of the Number of Individuals in Animal Species Living Together, J. Conseil 3 (1928), 3-51. https://doi.org/10.1093/icesjms/3.1.3.

[27] F.H. Maghool, R.K. Naji, The Dynamics of a Tritrophic Leslie-Gower Food-Web System with the Effect of Fear, J. Appl. Math. 2021 (2021), 2112814. https://doi.org/10.1155/2021/2112814.

[28] B. Das, N. Santra, G. Samanta, Exploring Dynamics of Predator-Prey Interactions: Fear, Toxicity, Carry Over and Environmental Fluctuations, Filomat 38 (2024), 11061-11083. https://doi.org/10.2298/fil2431061d.

[29] J. Liu, B. Liu, P. Lv, T. Zhang, An Eco-Epidemiological Model with Fear Effect and Hunting Cooperation, Chaos, Solitons Fractals 142 (2021), 110494. https://doi.org/10.1016/j.chaos.2020.110494.

[30] N. Sk, S. Pal, Dynamics of an Infected Prey–Generalist Predator System with the Effects of Fear, Refuge and Harvesting: Deterministic and Stochastic Approach, Eur. Phys. J. Plus 137 (2022), 138. https://doi.org/10.1140/epjp/s13360-022-02348-9.

[31] A. Sha, J. Chattopadhyay, Dynamical Study of Fear Effect In Prey–Predator Model With Disease In Predator, J. Biol. Syst. 31 (2023), 1319-1340. https://doi.org/10.1142/s0218339023500444.

[32] B. Mondal, A. Sarkar, N. Sk, Treatment of Infected Predators Under the Influence of Fear-Induced Refuge, Sci. Rep. 13 (2023), 16623. https://doi.org/10.1038/s41598-023-43021-0.

[33] P. Turchin, Complex Population Dynamics, Princeton University Press, (2003).
[34] J.D. Murray, Mathematical Biology I. An Introduction, Springer, (2002).
[35] C.S. Holling, The Components of Predation as Revealed by a Study of Small-Mammal Predation of the European Pine Sawfly, Can. Entomol. 91 (1959), 293-320. https://doi.org/10.4039/ent91293-5.
[36] C.S. Holling, Some Characteristics of Simple Types of Predation and Parasitism, Can. Entomol. 91 (1959), 385-398. https://doi.org/10.4039/ent91385-7.
[37] J.R. Beddington, Mutual Interference Between Parasites or Predators and Its Effect on Searching Efficiency, J. Anim. Ecol. 44 (1975), 331-340. https://doi.org/10.2307/3866.
[38] D.L. DeAngelis, R.A. Goldstein, R.V. O'Neill, A Model for Trophic Interaction, Ecology 56 (1975), 881-892.
[39] R. Arditi, L.R. Ginzburg, Coupling in Predator-Prey Dynamics: Ratio-Dependence, J. Theor. Biol. 139 (1989), 311-326. https://doi.org/10.1016/s0022-5193(89)80211-5.
[40] H.S. Wu, F.M. Zhang, L.S. Wu, New Swarm Intelligence Algorithm-Wolf Pack Algorithm, Syst. Eng. Electron. 35 (2013), 204-212.
[41] Y.L. Fang, X.L. Yang, C. Xiao, Z.N. Zhang, Electroantennogram Responses of Female Helicoverpa Armigera to the Volatile Components of Wheat Blossom, Acta Entomol. Sin. 47 (2004), 269-272.
[42] P.X. Shen, Y.K. Xue, Analysis of Model in a Predator-Prey System with Refuge Under the Impact of Odor, J Chongqing Univ. Technol. (Nat. Sci) 32 (2018), 205-211.
[43] W. Xu, D. Wu, J. Gao, C. Shen, Mechanisms of Stable Species Coexistence in Food Chain Systems: Strength of Odor Disturbance and Group Defense, Chaos Solitons Fractals: X 8 (2022), 100073. https://doi.org/10.1016/j.csfx.2022.100073.
[44] D. Bhattacharjee, D. Das, D.J. Sarma, S. Acharjee, Understanding the Influence of Prey Odour in Predator Species: A Three-Species Food Chain Study, Commun. Math. Biol. Neurosci. 2023 (2023), 93. https://doi.org/10.28919/cmbn/8099.
[45] F. Chen, On a Nonlinear Nonautonomous Predator–Prey Model with Diffusion and Distributed Delay, J. Comput. Appl. Math. 180 (2005), 33-49. https://doi.org/10.1016/j.cam.2004.10.001.
[46] L. Perko, Differential Equations and Dynamical Systems, 3rd edition, Springer, New York, (2001).
[47] K. Hattaf, A New Class of Generalized Fractal and Fractal-Fractional Derivatives with Non-Singular Kernels, Fractal Fract. 7 (2023), 395. https://doi.org/10.3390/fractalfract7050395.
[48] K. Hattaf, A New Mixed Fractional Derivative with Applications in Computational Biology, Computation 12 (2024), 7. https://doi.org/10.3390/computation12010007.